

Algorithms for the Laplace-Stieltjes Transforms of First Return Times for Stochastic Fluid Flows

Nigel G. Bean · Małgorzata M. O'Reilly ·
Peter G. Taylor.

Received: date / Accepted: date

Abstract We derive several algorithms, including quadratically convergent algorithms, which can be used to calculate the Laplace-Stieltjes transforms of the time taken to return to the initial level in the Markovian stochastic fluid flow model. We give physical interpretations of the algorithms and consider their numerical analysis. The numerical performance of the algorithms, which depends on the physical properties of the process, is discussed and illustrated with simple examples.

Besides the powerful algorithms, this paper contributes interesting theoretical results. In particular, the methodology for constructing these algorithms is a valuable contribution to the theory of fluid flow models. Moreover, useful physical interpretations of the algorithms, and related expressions, given in terms of the fluid flow model, can assist in further analysis and help in a better understanding of the model.

Keywords Markovian fluid model · Ricatti equation · Newton's method · Logarithmic-Reduction algorithm · Cyclic-Reduction algorithm

The authors would like to thank the Australian Research Council for funding this research through Discovery Project DP0209921.

Nigel G. Bean
Applied Mathematics, University of Adelaide, SA 5005, Australia
Tel.: +61-8-8303-3797
Fax: +61-8-8303-3866
E-mail: nigel.bean@adelaide.edu.au

Małgorzata M. O'Reilly
Department of Mathematics, University of Tasmania, Tas 7001, Australia Tel.: +61-3-6226-2405
Fax: +61-3-6226-2410
E-mail: fauthor@example.com

Peter G. Taylor
Department of Mathematics and Statistics, University of Melbourne, Vic 3010, Australia Tel.: +61-3-8344-6045
Fax: +61-3-8344-4599
E-mail: p.taylor@ms.unimelb.edu.au

1 Introduction

We consider the Markov stochastic fluid flow model $(\widehat{M}(t), \varphi(t))$. Let $\widehat{M}(t) \in \mathbb{R}^+$ denote the level of fluid in a container at time t . The rate of increase of $\widehat{M}(t)$ is determined by the state $\varphi(t)$ of a continuous-time Markov chain with finite state space \mathcal{S} and generator $\mathcal{T} = [\mathcal{T}_{ij}]$. Specifically, when $\widehat{M}(t) > 0$, the rate of increase of $\widehat{M}(t)$ is equal to $c_{\varphi(t)}$, which may be positive, negative or zero. If $\widehat{M}(t) = 0$, then $\widehat{M}(t)$ can change only if $c_{\varphi(t)} > 0$, in which case the rate of increase is $c_{\varphi(t)}$. Let \mathcal{S}_1 , \mathcal{S}_2 and \mathcal{S}_0 denote the sets of states, or *phases*, $i \in \mathcal{S}$ for which $c_i > 0$, $c_i < 0$ and $c_i = 0$, respectively. We partition the generator \mathcal{T} according to $\mathcal{S} = \mathcal{S}_1 \cup \mathcal{S}_2 \cup \mathcal{S}_0$ so that

$$\mathcal{T} = \begin{bmatrix} T_{11} & T_{12} & T_{10} \\ T_{21} & T_{22} & T_{20} \\ T_{01} & T_{02} & T_{00} \end{bmatrix}.$$

Further, let C_1 be a diagonal matrix such that $[C_1]_{ii} = c_i$ for all $i \in \mathcal{S}_1$, C_2 be a diagonal matrix such that $[C_2]_{ii} = -c_i$ for all $i \in \mathcal{S}_2$, and let

$$C = \begin{bmatrix} C_1 & 0 & 0 \\ 0 & C_2 & 0 \\ 0 & 0 & I \end{bmatrix}.$$

This notation is not a natural choice, as the rates c_i for $i \in \mathcal{S}_0$ are zero, but we use it here to be consistent with [3].

Let $\theta(x) = \inf\{t > 0 : \widehat{M}(t) = x\}$ be the first passage time to level x . We define, for s with $\text{Re}(s) \geq 0$, the following matrix $\widehat{\Psi}(s)$. For $i \in \mathcal{S}_1$ and $j \in \mathcal{S}_2$, $[\widehat{\Psi}(s)]_{ij}$ is given by the conditional expectation

$$[\widehat{\Psi}(s)]_{ij} = E[e^{-s\theta(x)} : \theta(x) < \infty, \varphi(\theta(x)) = j | \widehat{M}(0) = x, \varphi(0) = i]. \quad (1)$$

In physical terms, $[\widehat{\Psi}(s)]_{ij}$ is the Laplace-Stieltjes transform of the time taken, starting from level x in phase i , to return to level x in finite time and do so in phase j , while avoiding levels below x .

The significance of this fluid model to the telecommunications performance analysis community has inspired a large amount of interest amongst researchers, and several results have been recently obtained by Ramaswami [22], da Silva Soares and Latouche [14, ?], Ahn and Ramaswami [2–4], Bean, O'Reilly and Taylor [8–10] and Bean and O'Reilly [7]. Amongst these results are formulae for various performance measures for the fluid flow model, which can be readily calculated once $\widehat{\Psi}(s)$ is known. Consequently, fast algorithms for the evaluation of $\widehat{\Psi}(s)$ are needed. One quadratically convergent algorithm for $\widehat{\Psi}(s)$ has been introduced by Ahn and Ramaswami in [3]. In this paper, we derive five quadratically convergent algorithms as well as nine linear algorithms which are interesting for theoretical reasons. We give the detailed analysis of these algorithms and discuss their performance via numerical examples.

Several of these algorithms, including one quadratically convergent algorithm, are obtained by simple transformations of the Riccati equation for $\widehat{\Psi}(s)$ [8],

$$Q_{12}(s) + Q_{11}(s)\widehat{\Psi}(s) + \widehat{\Psi}(s)Q_{22}(s) + \widehat{\Psi}(s)Q_{21}(s)\widehat{\Psi}(s) = 0, \quad (2)$$

where

$$\begin{aligned} Q_{11}(s) &= C_1^{-1}[(T_{11} - sI) - T_{10}(T_{00} - sI)^{-1}T_{01}], \\ Q_{22}(s) &= C_2^{-1}[(T_{22} - sI) - T_{20}(T_{00} - sI)^{-1}T_{02}], \\ Q_{12}(s) &= C_1^{-1}[T_{12} - T_{10}(T_{00} - sI)^{-1}T_{02}], \quad \text{and} \\ Q_{21}(s) &= C_2^{-1}[T_{21} - T_{20}(T_{00} - sI)^{-1}T_{01}]. \end{aligned} \quad (3)$$

The remaining quadratically convergent algorithms are obtained by applying the Logarithmic Reduction algorithm [20] and the Cyclic Reduction algorithm [12], respectively, to each of two appropriately defined sets of matrices. One of these algorithms produces an algorithm that is essentially equivalent to the one produced by an algorithm introduced by Ahn and Ramaswami [3].

This work is an extension of a previous paper [9], in which we derived and analyzed several algorithms for the calculation of the matrix $\Psi = \hat{\Psi}(0)$, which records first return probabilities. Here, we give the results for the Laplace-Stieltjes transforms of first return times as well as several new algorithms for the matrix $\hat{\Psi}(s)$. We apply these results to calculate the probability density of the first return time.

The paper is organized as follows. In Section 2 we introduce the algorithms. In Section 3 we give their physical interpretations and prove their convergence to $\hat{\Psi}(s)$. The numerical complexity of each of the algorithms is established in Section 4, while the performance of the algorithms is discussed and illustrated with simple examples in Section 5. An application to calculating the probability density of the first return time to the initial level is presented in Section 6. This is followed by concluding remarks in Section 7.

We believe that this paper is a valuable contribution to the theory of stochastic fluid flow models. From the numerical point of view, we construct several powerful algorithms, which are useful for the calculation of important performance measures that involve $\hat{\Psi}(s)$. From the theoretical point of view, we contribute a useful methodology, a thorough analysis, and interesting insights such as the relationship between the algorithms and their physical interpretations. We emphasize that all physical interpretations are given within the fluid flow model. This direct treatment of the model provides a valuable tool that can greatly assist in a better understanding of the fluid flow model.

2 Algorithms

In this section we introduce all the algorithms. Their detailed analysis and proofs of their convergence to $\hat{\Psi}(s)$ are given in the next section. Here, we focus mainly on the construction of the algorithms and on how they correspond to results in the literature. Similarly to [9], we begin by writing the Riccati equation for the matrix of interest in several different forms and introducing corresponding iterations. For example, we can write (2) as

$$Q_{11}(s)\hat{\Psi}(s) + \hat{\Psi}(s)Q_{22}(s) = -Q_{12}(s) - \hat{\Psi}(s)Q_{21}(s)\hat{\Psi}(s).$$

A corresponding iteration is constructed by setting $\hat{\Psi}(s, 0) = 0$, and then, for $n \geq 1$,

$$(A1.) \quad Q_{11}(s)\hat{\Psi}(s, n+1) + \hat{\Psi}(s, n+1)Q_{22}(s) = -Q_{12}(s) - \hat{\Psi}(s, n)Q_{21}(s)\hat{\Psi}(s, n).$$

In a similar manner, by rearranging (2), we construct

$$\begin{aligned}
(\mathbf{A2.}) \quad & Q_{11}(s)\widehat{\Psi}(s, n+1) + \widehat{\Psi}(s, n+1)\left(Q_{22}(s) + Q_{21}(s)\widehat{\Psi}(s, n)\right) = -Q_{12}(s), \\
(\mathbf{A3.}) \quad & \left(Q_{11}(s) + \widehat{\Psi}(s, n)Q_{21}(s)\right)\widehat{\Psi}(s, n+1) + \widehat{\Psi}(s, n+1)Q_{22}(s) = -Q_{12}(s), \text{ and} \\
(\mathbf{A4.}) \quad & \left(Q_{11}(s) + \widehat{\Psi}(s, n)Q_{21}(s)\right)\widehat{\Psi}(s, n+1) + \widehat{\Psi}(s, n+1)\left(Q_{22}(s) + Q_{21}(s)\widehat{\Psi}(s, n)\right) = \\
& -Q_{12}(s) + \widehat{\Psi}(s, n)Q_{21}(s)\widehat{\Psi}(s, n).
\end{aligned}$$

By letting $s = 0$ in Algorithms 1 to 4, we obtain the fixed-point iteration FP3 [17], First-Exit algorithm [9], Last-Entrance algorithm [9] and Newton's method [17], respectively, which are algorithms for Ψ . The analysis and comparison of these algorithms were given in [9]. Note the symmetry between the Algorithms 2 and 3. We shall say that one is the *dual* of the other. Algorithm 4 has a more complicated form than the three other algorithms. As we shall see in the next section, Algorithm 4 is quadratically convergent.

The family of algorithms **(A5.)** to **(A10.)** below are based on the embedded jump chain and the uniformized chain (Jensen [18]), applied to the Markov Chain underlying the fluid flow process. Similar conditioning was used earlier by Asmussen [5] in the construction of the algorithms for Ψ . The algebraic construction is presented here. Details of the physical interpretations of these algorithms are given in Section 3.2. Let

$$Q(s) = \begin{bmatrix} Q_{11}(s) & Q_{12}(s) \\ Q_{21}(s) & Q_{22}(s) \end{bmatrix},$$

and $Q = Q(0)$. Also, let $A_{i\bullet}$ and $A_{\bullet j}$ be the i -th row and the j -th column of the matrix A , respectively. We note that, by considering one row at a time, the equation (2) can be written in the form

$$\left[-\mathbf{Z}_i\widehat{\Psi}(s)\right]_{i\bullet} + \left[\widehat{\Psi}(s)\left(Q_{22}(s) + Q_{21}(s)\widehat{\Psi}(s)\right)\right]_{i\bullet} = \left[-Q_{12}(s) - \left(Q_{11}(s) + \mathbf{Z}_i\right)\widehat{\Psi}(s)\right]_{i\bullet}, \quad (4)$$

where \mathbf{Z}_i is an arbitrary matrix dependent on i , and then a corresponding iteration can be introduced. When \mathbf{Z}_i is replaced by $z_i I$, where z_i is some constant and for appropriate sized matrices I , then (4) can be written in the form,

$$\left[\widehat{\Psi}(s)\right]_{i\bullet} = \left[\left(Q_{12}(s) + \left(Q_{11}(s) + z_i I\right)\widehat{\Psi}(s)\right)\left(z_i I - Q_{22}(s) - Q_{21}(s)\widehat{\Psi}(s)\right)^{-1}\right]_{i\bullet}, \quad (5)$$

which leads to a more convenient iteration. To guarantee the convergence to $\widehat{\Psi}(s)$, we choose a particular value of z_i , which leads to a physical interpretation of the iteration, from which the convergence will follow. For example, with $z_i = \left(\frac{-\mathcal{T}_{ii}+s}{c_i}\right)$, an iteration based on (4) becomes

$$\begin{aligned}
(\mathbf{A5a.}) \quad & \left[-\left(\frac{-\mathcal{T}_{ii}+s}{c_i}\right)\widehat{\Psi}(s, n+1)\right]_{i\bullet} + \left[\widehat{\Psi}(s, n+1)\left(Q_{22}(s) + Q_{21}(s)\widehat{\Psi}(s, n)\right)\right]_{i\bullet} = \left[-Q_{12}(s) - \right. \\
& \left.\left(Q_{11}(s) + \left(\frac{-\mathcal{T}_{ii}+s}{c_i}\right)I\right)\widehat{\Psi}(s, n)\right]_{i\bullet} \quad \text{for } i \in \mathcal{S}_1,
\end{aligned}$$

which can be written in the form

$$\begin{aligned}
(\mathbf{A5.}) \quad & \left[\widehat{\Psi}(s, n+1)\right]_{i\bullet} = \left[\left(Q_{12}(s) + \left(Q_{11}(s) + \left(\frac{-\mathcal{T}_{ii}+s}{c_i}\right)I\right)\widehat{\Psi}(s, n)\right) \times \right. \\
& \left.\left(\left(\frac{-\mathcal{T}_{ii}+s}{c_i}\right)I - Q_{22}(s) - Q_{21}(s)\widehat{\Psi}(s, n)\right)^{-1}\right]_{i\bullet} \quad \text{for } i = 1 \in \mathcal{S}_1.
\end{aligned}$$

By letting $s = 0$ in Algorithm 5, we obtain Asmussen's iteration in [5, Theorem 3.1], a linear algorithm for Ψ , the analysis of which was given in [8]. In this sense Algorithm 5 is a generalization of Asmussen's iteration. In an analogous manner we obtain an algorithm dual to Algorithm 5, in which at every step the j -th column for $j \in \mathcal{S}_2$ is calculated using

$$(A6.) \quad \left[\hat{\Psi}(s, n+1) \right]_{\bullet j} = \left[\left(\left(\frac{-\mathcal{T}_{jj}+s}{c_j} \right) I - Q_{11}(s) - \hat{\Psi}(s, n) Q_{21}(s) \right)^{-1} \times \right. \\ \left. \left(Q_{12}(s) + \hat{\Psi}(s, n) \left(Q_{22}(s) + \left(\frac{-\mathcal{T}_{jj}+s}{c_j} \right) I \right) \right) \right]_{\bullet j} \quad \text{for } j \in \mathcal{S}_2.$$

Let $\vartheta \geq \max_i \{-[C^{-1}T]_{ii}\}$. By the physical interpretations in the next section, this choice of the lower bound for ϑ guarantees the convergence of the algorithms below, which otherwise may be unstable. By taking $\mathbf{Z}_i = \vartheta I + sC_1^{-1}$ in (4) and constructing the corresponding iteration, we arrive at

$$(A7.) \quad -(\vartheta I + sC_1^{-1})\hat{\Psi}(s, n+1) + \hat{\Psi}(s, n+1) \left(Q_{22}(s) + Q_{21}(s)\hat{\Psi}(s, n) \right) = \\ -Q_{12}(s) - \left(Q_{11}(s) + (\vartheta I + sC_1^{-1}) \right) \hat{\Psi}(s, n),$$

together with its dual

$$(A8.) \quad \left(Q_{11}(s) + \hat{\Psi}(s, n) Q_{21}(s) \right) \hat{\Psi}(s, n+1) - \hat{\Psi}(s, n+1) (\vartheta I + sC_2^{-1}) = \\ -Q_{12}(s) - \hat{\Psi}(s, n) \left((\vartheta I + sC_2^{-1}) + Q_{22}(s) \right).$$

A convenient form based on (5) cannot be introduced for Algorithms 7 and 8. However, by taking $\mathbf{Z}_i = \vartheta I$, we arrive at

$$(A9.) \quad \hat{\Psi}(s, n+1) = \left(Q_{12}(s) + \left(Q_{11}(s) + \vartheta I \right) \hat{\Psi}(s, n) \right) \times \\ \left(\vartheta I - Q_{22}(s) - Q_{21}(s)\hat{\Psi}(s, n) \right)^{-1}$$

and its dual

$$(A10.) \quad \hat{\Psi}(s, n+1) = \left(\vartheta I - Q_{11}(s) - \hat{\Psi}(s, n) Q_{21}(s) \right)^{-1} \times \\ \left(Q_{12}(s) + \hat{\Psi}(s, n) \left(Q_{22}(s) + \vartheta I \right) \right),$$

which are more attractive numerically. In Section 3.2 we explain how Algorithm 7 is a generalization of the iteration in Asmussen [5, Theorem 3.2] and Algorithm 8 is a generalization of the iteration in [8, equation (19)]. Also, we explain there how Algorithms 9 and 10 relate to Algorithms 7 and 8. Both Algorithms 9 and 10 play an important part in the physical interpretation of the four quadratically convergent algorithms constructed next.

The construction of the algorithms below is more complicated than in the case of Algorithms 1-10. In order to fully appreciate the methodology of this construction, the reader is referred to the physical interpretations and the analysis given in the subsequent section. Let $P(s) = I + \frac{1}{\vartheta}Q(s)$ be partitioned in a manner analogous to the

partitioning of $Q(s)$. Define two sets of matrices

$$A_0(s) = \begin{bmatrix} \frac{1}{2}I & 0 \\ 0 & 0 \end{bmatrix}, \quad A_1(s) = \begin{bmatrix} \frac{1}{2}P_{11}(s) & 0 \\ P_{21}(s) & 0 \end{bmatrix}, \quad A_2(s) = \begin{bmatrix} 0 & \frac{1}{2}P_{12}(s) \\ 0 & P_{22}(s) \end{bmatrix}, \quad (6)$$

and

$$A'_0(s) = \begin{bmatrix} P_{11}(s) & P_{12}(s) \\ 0 & 0 \end{bmatrix}, \quad A'_1(s) = \begin{bmatrix} 0 & 0 \\ \frac{1}{2}P_{21}(s) & \frac{1}{2}P_{22}(s) \end{bmatrix}, \quad A'_2(s) = \begin{bmatrix} 0 & 0 \\ 0 & \frac{1}{2}I \end{bmatrix}. \quad (7)$$

For general (complex) s , we shall see that the matrix $\hat{\Psi}(s)$ can be calculated by algebraically applying any algorithm for the evaluation of the G -matrix in a quasi-birth-and-death process QBD to either of the two sets of matrices in (6) and (7). This approach was first used by Ahn and Ramaswami [3] where they algebraically applied the Logarithmic Reduction algorithm [17] algorithm to the set of matrices given in (21) below. These matrices are closely related to the matrices given in (7), except that for the matrices given in (7) the effects of excursions to the set \mathcal{S}_0 have been captured in $P(s)$ itself, rather than being modelled explicitly.

When s is real and positive, the entries in the matrices in (6) and (7) still have direct probabilistic interpretations (even if as defective distributions) and so the convergence of any known QBD algorithm is still assured. However, in the case of general complex s (with non-negative real part) the entries in the matrices no longer have a direct physical interpretation as probabilities and so there is no guarantee of convergence of any of the known QBD algorithms. Ahn and Ramaswami [3] directly established convergence of their approach in the general setting of complex s . In this paper, we show the convergence of the algorithms by proving equivalence between known iterations of certain earlier algorithms to iterations of these algorithms.

Below we summarize four algorithms constructed by algebraically applying the Logarithmic Reduction algorithm [20] and the Cyclic Reduction algorithm [12], respectively, to each of the sets of matrices in (6)-(7). We assume that G^\bullet is partitioned in a way analogous to the partitioning of the matrix $Q(s)$. Algorithm 13 and Algorithm 3 of Ahn and Ramaswami [3] both lead to the calculation of the same matrix $\hat{\Psi}(s, n)$ at the n -th step (and hence the same approximation of the matrix $\hat{\Psi}(s)$). The proof of this equivalence is given in the next section. Due to its slightly smaller numerical complexity per iteration (see Section 4 for details), Algorithm 13 is a better performer than the algorithm given in [3]. Algorithm 11 is the dual of Algorithm 13, and Algorithm 12 is the dual of Algorithm 14. The details of this duality are given in the next section.

$$\begin{aligned} \text{(A11.) } H^\bullet &:= (I - A_1(s))^{-1} A_0(s); \\ L^\bullet &:= (I - A_1(s))^{-1} A_2(s); \\ G^\bullet &:= L^\bullet; \\ T &:= H^\bullet; \\ \text{repeat} \\ U^\bullet &:= H^\bullet L^\bullet + L^\bullet H^\bullet; \\ M &:= (H^\bullet)^2; \\ L^\bullet &:= (I - U^\bullet)^{-1} M; \end{aligned}$$

$$\begin{aligned}
G^{\bullet\bullet} &= G^\bullet; \\
G^\bullet &:= G^\bullet + TL^\bullet; \\
T &:= TH^\bullet; \\
\hat{\Psi}(s) &\approx G_{12}^\bullet;
\end{aligned}$$

until a stopping criterion is met.

(A12.) $A_0^\bullet = A_0(s);$
 $A_1^\bullet = A_1(s);$
 $A_2^\bullet = A_2(s);$
 $\hat{A}_1^\bullet = A_1(s);$
 $G^\bullet = (I - \hat{A}_1^\bullet)^{-1} A_2(s);$
repeat
 $A_1^\bullet = A_1^\bullet + A_0^\bullet (I - \hat{A}_1^\bullet)^{-1} A_2^\bullet;$
 $A_2^\bullet = A_2^\bullet (I - \hat{A}_1^\bullet)^{-1} A_2^\bullet;$
 $A_0^\bullet = A_0^\bullet (I - \hat{A}_1^\bullet)^{-1} A_0^\bullet;$
 $\hat{A}_1^\bullet = \hat{A}_1^\bullet + A_0^\bullet (I - \hat{A}_1^\bullet)^{-1} A_2^\bullet;$
 $G^{\bullet\bullet} = G^\bullet;$
 $G^\bullet = (I - \hat{A}_1^\bullet)^{-1} A_2(s);$
 $\hat{\Psi}(s) \approx G_{12}^\bullet;$

until a stopping criterion is met.

- (A13.) Apply Algorithm 11, replacing the matrices (6) with (7), and changing the last step in each iteration to $\hat{\Psi}(s) \approx P_{11}(s)G_{12}^\bullet + P_{12}(s)G_{22}^\bullet$.
(A14.) Apply Algorithm 12, replacing the matrices (6) with (7), and changing the last step in each iteration to $\hat{\Psi}(s) \approx P_{11}(s)G_{12}^\bullet + P_{12}(s)G_{22}^\bullet$.

As a stopping criterion, the condition $\max_{i,j} |[G^\bullet]_{ij} - [G^{\bullet\bullet}]_{ij}| \leq \epsilon$ can be used, for the desired maximum error $\epsilon > 0$. The approximation of the matrix $\hat{\Psi}(s)$ obtained after n iterations of Algorithms 11, 12, 13 and 14, respectively, shall be denoted as $\hat{\Psi}(s, n)$, consistently with the notation for other algorithms.

3 Physical interpretations

The physical interpretations of Algorithms 3, 6, 8, 10, 13 and 14 follow by symmetry from the physical interpretations of their duals, that is Algorithms 2, 5, 7, 9, 11 and 12, respectively. To determine the physical interpretations of Algorithms 2 and 5 we condition on the first level that the process leaves a given state/set of states, respectively, while in Algorithms 3 and 6 we condition on the last level that the process enters a given state/set of states, respectively. In Algorithms 7 and 9 we condition on the first clock ring at which the process leaves a given state, while in Algorithms 8 and 10 we condition on the last clock ring at which the process enters a given state, in an appropriate uniformization scheme. The iterations of Algorithms 11 and 13 are then obtained in terms of appropriate iterations of Algorithms 10 and 9, respectively. The physical interpretations of Algorithms 12 and 14 are largely similar to those of Algorithms 11 and 13, respectively.

The physical interpretations of Algorithms 1-5 and 11-12 have been given in [8] for the case $s = 0$ in the model with $c_i = \pm 1$ for all $i \in \mathcal{S}$. The physical interpretations of these algorithms for the case $s = 0$ in the *general* model with $c_i \in \mathbb{R}$, $i \in \mathcal{S}$, follows

from [9] by replacing the matrix \mathcal{T} with Q and by interpreting y , which appears in the integrals in the formulae for these algorithms, as the fluid level.

In this interpretation, at each iteration of the algorithms the matrix $\hat{\Psi}(0, n)$ records the total probability mass of certain sample paths. For $i \in \mathcal{S}_1$, $j \in \mathcal{S}_2$, and a given algorithm, let $[\Omega]_{ij}$ be the set of sample paths that contribute to $[\hat{\Psi}(0)]_{ij}$ and let $[\Omega_n]_{ij}$ be the set of sample paths that contribute to $[\hat{\Psi}(0, n)]_{ij}$. The physical interpretation of the n -th iteration of this algorithm for *complex* s , $\text{Re}(s) > 0$, is that $[\hat{\Psi}(s, n)]_{ij}$ is the Laplace-Stieltjes transform of the time taken to traverse paths in $[\Omega_n]_{ij}$. The details are given below.

Note that the expressions for $\hat{\Psi}(s, n+1)$ in Algorithms 1-10 introduced in the previous section, can be written as linear equations of the form

$$AX + XB = -C,$$

where $X = \hat{\Psi}(s, n+1)$ and A , B and C are coefficient matrices given in terms of $\hat{\Psi}(s, n)$. By [11, Theorem 9.2], whenever the spectra of the matrices A and B are contained in the open left half plane, this linear form is equivalent to the integral form

$$X = \int_0^\infty e^{Au} C e^{Bu} du.$$

While the linear form for each algorithm is easier to implement, the integral form is easier to understand in terms of the physical interpretations, and so we will use the integral form in this section. The physical interpretations that we discuss will justify the assumption about the spectra of the matrices A and B , and hence the equivalence of the two forms, in all cases below.

3.1 Algorithms 1-4

The integral forms of Algorithms 1-4 are

- (A1.) $\hat{\Psi}(s, n+1) = \int_0^\infty e^{Q_{11}(s)y} (Q_{12}(s) + \hat{\Psi}(s, n)Q_{21}(s)\hat{\Psi}(s, n)) e^{Q_{22}(s)y} dy,$
- (A2.) $\hat{\Psi}(s, n+1) = \int_0^\infty e^{Q_{11}(s)y} Q_{12}(s) e^{(Q_{22}(s)+Q_{21}(s)\hat{\Psi}(s, n))y} dy,$
- (A3.) $\hat{\Psi}(s, n+1) = \int_0^\infty e^{(Q_{11}(s)+\hat{\Psi}(s, n)Q_{21}(s))y} Q_{12}(s) e^{Q_{22}(s)y} dy,$
- (A4.) $\hat{\Psi}(s, n+1) = \int_0^\infty e^{(Q_{11}(s)+\hat{\Psi}(s, n)Q_{21}(s))y} \times$
 $(Q_{12}(s) - \hat{\Psi}(s, n)Q_{21}(s)\hat{\Psi}(s, n)) e^{(Q_{22}(s)+Q_{21}(s)\hat{\Psi}(s, n))y} dy.$

The physical interpretations of Algorithms 1-4 follow from the physical interpretation of the matrices appearing under the integrals in the above formulae. In [8], we gave the physical interpretations of matrices $e^{Q_{11}(s)y}$, $e^{Q_{22}(s)y}$, $Q_{12}(s)$ and $Q_{21}(s)$. In [10], we gave the physical interpretation of the matrix $e^{(Q_{22}(s)+Q_{21}(s)\hat{\Psi}(s))y}$. From this, the physical interpretation of the matrix $e^{(Q_{22}(s)+Q_{21}(s)\hat{\Psi}(s, n))y}$ follows by restricting sets $[\Omega]_{kl}$ to $[\Omega_n]_{kl}$, $k \in \mathcal{S}_1$, $\ell \in \mathcal{S}_2$. That is, it follows by placing a restriction on the shape of return paths to the original level. Then, the physical interpretation of the matrix $e^{(Q_{11}(s)+\hat{\Psi}(s, n)Q_{21}(s))y}$ follows by symmetry and a time reversal argument.

The physical interpretations of each of Algorithms 1-4 are similar in the sense that a sample path contributing to $\hat{\Psi}(s, n+1)$ can be split into three stages, in each of these algorithms. The first and the third stages correspond to the exponential matrices under the integral (in the formula for a given algorithm), on the left and on the right

hand side, respectively. The first stage starts from level zero and ends at level y , while the third stage starts from level y and ends at level zero. The second stage, which corresponds to the expression in the middle of the formula, starts from level y and ends at level y .

The difference between the algorithms lies in the shape of paths corresponding to the three stages, and in particular, in the complexity of the shape of paths corresponding to the first and third stage. Algorithm 1 has the least complex form, while Algorithm 4 has the most complex form.

Here we shall give the details of the physical interpretation of Algorithm 4. We omit the details of the physical interpretations of Algorithms 1-3, as they can be obtained in a similar way. In Algorithm 4, in sample paths contributing to the $(n+1)$ -st iteration,

- the first stage corresponds to the matrix $e^{(Q_{11}(s) + \hat{\Psi}(s,n)Q_{21}(s))y}$. The physical interpretation of this stage is dual to the physical interpretation of the third stage, given below. The first stage starts at level zero in some phase $i \in \mathcal{S}_1$ and ends at level y in some phase $k \in \mathcal{S}_1$. During this time, if at some level $z \in (0, y)$ an event occurs such that the process moves from some phase in \mathcal{S}_2 to some phase in \mathcal{S}_1 directly, or after visiting the set \mathcal{S}_0 first, then such an event is preceded directly by a return path to level z which must be in the set $[\Omega_n]_{\nu\mu}$ for some $\nu \in \mathcal{S}_1$ and $\mu \in \mathcal{S}_2$. That is, during this stage, any return path to a level $z \in (0, y)$ must be in the set $[\Omega_n]_{\nu\mu}$ for some $\nu \in \mathcal{S}_1$ and $\mu \in \mathcal{S}_2$.
- The second stage corresponds to $(Q_{12}(s) - \hat{\Psi}(s,n)Q_{21}(s)\hat{\Psi}(s,n))$. In this stage, either
 - the process makes a single transition from k to some $\ell \in \mathcal{S}_2$, or
 - the process makes a single transition from k to some phase $k' \in \mathcal{S}_0$, spends some time in the set \mathcal{S}_0 and then makes a single transition from the set \mathcal{S}_0 to some phase $\ell \in \mathcal{S}_2$.

The term $(-\hat{\Psi}(s,n)Q_{21}(s)\hat{\Psi}(s,n))$ is a corrective term which prevents multiple counting of the same sample path, by an argument analogous to that used for the physical interpretation of Newton's method in [9].

- The third stage corresponds to the matrix $e^{(Q_{22}(s) + Q_{21}(s)\hat{\Psi}(s,n))y}$. The process, starting from level y in phase ℓ , first drains to level zero and does so in phase j . During this time, if at some level $z \in (0, y)$ an event occurs such that the process moves from some phase in \mathcal{S}_2 to some phase in \mathcal{S}_1 directly, or after visiting the set \mathcal{S}_0 first, then such an event is followed directly by a return path to level z which must be in the set $[\Omega_n]_{\nu\mu}$ for some $\nu \in \mathcal{S}_1$ and $\mu \in \mathcal{S}_2$.

3.2 Algorithms 5-10

The physical interpretations for Algorithms 6, 8 and 10 follow by symmetry from the physical interpretations of Algorithms 5, 7 and 9, respectively, and so we give here the physical interpretations of Algorithms 5, 7 and 9 only. Below, we derive the physical interpretation of Algorithm 5 by considering the embedded jump chain of the Markov Chain underlying the fluid flow process and conditioning on the first jump. The physical interpretation of Algorithm 7 follows by applying uniformization (see [18]) to the underlying Markov Chain and conditioning on the first clock ring. The physical interpretation of Algorithm 9 is then obtained by calculating hitting probabilities, instead of

the Laplace-Stieltjes transforms, of a related process with a modified generator, using Algorithm 7.

In the integral form Algorithm 5 can be written as

$$(A5) \quad \left[\widehat{\Psi}(s, n+1) \right]_{i\bullet} = \int_0^\infty e^{-(\frac{-\mathcal{T}_{ii}+s}{c_i})y} \times \\ \times \left[Q_{12}(s) + \left(Q_{11}(s) + (\frac{-\mathcal{T}_{ii}+s}{c_i})I \right) \widehat{\Psi}(s, n) \right]_{i\bullet} e^{(Q_{22}(s)+Q_{21}(s)\widehat{\Psi}(s,n))y} dy.$$

We first establish the physical interpretations of the matrices under the integral in Algorithm 5. Assume that the process starts in phase $i \in \mathcal{S}_1$ at level zero. The probability that the process stays in i at least until reaching level y is $e^{(\mathcal{T}_{ii}/c_i)y}$, the associated time taken is (y/c_i) , and so the corresponding Laplace-Stieltjes transform conditioned on this event occurring is $e^{-(y/c_i)s}$, and the product of these is

$$e^{-(\frac{-\mathcal{T}_{ii}+s}{c_i})y}.$$

The physical interpretation of the exponential matrix on the right hand side has been given in the previous section. The physical interpretation of the i -th row of $\left(Q_{11}(s) + (\frac{-\mathcal{T}_{ii}+s}{c_i})I \right)$ follows from the physical interpretation of the i -th row of $Q_{11}(s)$, given in [8], by restricting the allowable transitions to those from i to $\mathcal{S} \setminus \{i\}$ only (and so, not allowing transitions from i to i). This follows from the fact that $[C_1^{-1}(T_{11} - sI) + (\frac{-\mathcal{T}_{ii}+s}{c_i})I]_{ii} = 0$ for all i . Specifically, in this physical interpretation, the process either makes a single transition to some phase in $\mathcal{S}_1 \setminus \{i\}$; or it makes a single transition to some phase in \mathcal{S}_0 , spends some time in the set \mathcal{S}_0 , and then makes a single transition from the set \mathcal{S}_0 to some phase in \mathcal{S}_1 .

We are now ready to give the physical interpretation of Algorithm 5. In this algorithm, in sample paths contributing to the i -th row of the $(n+1)$ -st iteration, the three following stages occur.

- The first stage corresponds to the scalar $e^{-(\frac{-\mathcal{T}_{ii}+s}{c_i})y}$. The process starting from level zero in phase $i \in \mathcal{S}_1$, remains in i , until reaching level y .
- In the second stage, corresponding to $Q_{12}(s) + \left(Q_{11}(s) + (c_i^{-1} - \mathcal{T}_{ii}I + sC_1^{-1}) \right) \widehat{\Psi}(s, n)$, either of the following alternatives may occur.
 - In the first alternative, corresponding to $Q_{12}(s)$, the process either makes a single transition to some phase $\ell \in \mathcal{S}_2$; or it makes a single transition to some phase in \mathcal{S}_0 , spends some time in the set \mathcal{S}_0 , and then makes a single transition from the set \mathcal{S}_0 to phase $\ell \in \mathcal{S}_2$.
 - In the second alternative, corresponding to $\left(Q_{11}(s) + (c_i^{-1} - \mathcal{T}_{ii}I + sC_1^{-1}) \right) \widehat{\Psi}(s, n)$, the process either makes a single transition to some phase in $\mathcal{S}_1 \setminus \{i\}$; or it makes a single transition to some phase in \mathcal{S}_0 , spends some time in the set \mathcal{S}_0 , and then makes a single transition from the set \mathcal{S}_0 to some phase \mathcal{S}_1 . Next, the process first returns to level y and does so in some phase $\ell \in \mathcal{S}_2$. This return path to level y must be in the set $[\Omega_n]_{\nu\mu}$ for some $\nu \in \mathcal{S}_1$ and $\mu \in \mathcal{S}_2$.
- In the third stage, corresponding to $e^{(Q_{22}(s)+Q_{21}(s)\widehat{\Psi}(s,n))y}$, starting from level y in phase $\ell \in \mathcal{S}_2$, the process first drains to level zero and does so in phase j . During this time, if at some level $z \in (0, y)$ an event occurs such that the process moves

from some phase in \mathcal{S}_2 to some phase in \mathcal{S}_1 directly, or after visiting the set \mathcal{S}_0 first, then such an event is followed directly by a return path to level z which must be in the set $[\Omega_n]_{\nu\mu}$ for some $\nu \in \mathcal{S}_1$ and $\mu \in \mathcal{S}_2$.

In short, we condition here on the first *level* that the process leaves phase i , at which point the process moves to some phase $j \in \mathcal{S}$ with probability $-\mathcal{T}_{ij}/\mathcal{T}_{ii}$. That is, we apply here the *embedded jump chain* of the continuous-time Markov Chain underlying the fluid flow process. A similar conditioning (on the first *time* the process leaves phase i) was earlier used by Asmussen [5, Theorem 3.1], in a simplified model (with $c_i = \pm 1$), for calculating probabilities. Here, we consider a general fluid model and calculate the Laplace-Stieltjes transforms of the time taken to traverse sample paths. In this sense, Algorithm 5 is a generalization of the algorithm in Theorem 3.1 in Asmussen.

Algorithm 7 follows from Algorithm 5 by the same argument by which the algorithm in Theorem 3.2 in [5] follows from the algorithm in Theorem 3.1 in [5], and in this sense Algorithm 7 is a generalization of the latter algorithm in Asmussen. Algebraically, Algorithm 7 follows from Algorithm 5 by replacing $-\mathcal{T}_{ii}$ by $\vartheta|c_i|$ for all $i \in \mathcal{S}_1 \cup \mathcal{S}_2$. Physically, the shapes of paths contributing to the n -th iteration in Algorithm 7 are analogous to the shapes of paths in Algorithm 5. However, now we assume that time is measured in a way according to the uniformization scheme introduced by Jensen [18], and a corresponding probability matrix of transitions is defined, which allows, on leaving some phase i , the possibility of coming back to i again. Specifically, as in [5], we assume that a Poisson clock rings at a rate $\vartheta[C]_{ii}$ when the process is in phase i . Then, the value of y at the first clock ring is exponentially distributed with rate ϑ , and state transitions occur according to the transition matrix $P = \vartheta^{-1}C^{-1}\mathcal{T} + I$. Here, we really are just describing the modulating process differently, using a discrete-time Markov Chain with jump levels that occur at a constant rate ϑ . The sojourn time distribution until the process actually leaves the phase is the same as before.

Below, by conditioning on the first level at which the clock first rings, we obtain an expression for $\hat{\Psi}(s)$, from which Algorithm 7 is derived.

Lemma 1 *The matrix $\hat{\Psi}(s)$ is given by*

$$\begin{aligned} \hat{\Psi}(s) &= \int_0^\infty e^{-(\vartheta I + sC_1^{-1})y} \times \\ &\times \left(Q_{12}(s) + \left(Q_{11}(s) + (\vartheta I + sC_1^{-1}) \right) \hat{\Psi}(s) \right) e^{(Q_{22}(s) + Q_{21}(s)\hat{\Psi}(s))y} dy. \end{aligned} \quad (8)$$

Proof Suppose that the process $(\hat{M}(t), \varphi(t))$ starts from level zero in phase $i \in \mathcal{S}_1$ and first returns to level zero in some phase $j \in \mathcal{S}_2$. We condition on the first level that the process leaves phase i . There are four alternatives:

1. In the first stage, there is no clock ring until the process reaches some level y , at which point it leaves i , and then instantly moves back to i . By multiplying the corresponding Laplace-Stieltjes transform, conditioned on this event occurring,

$$e^{-s \frac{y}{c_i}}$$

by the probability density of this event

$$\vartheta e^{-\vartheta y} \left(\frac{\mathcal{T}_{ii}}{\vartheta c_i} + 1 \right),$$

we obtain

$$e^{-(\vartheta + sc_i^{-1})y} \left(c_i^{-1} \mathcal{T}_{ii} + \vartheta \right). \quad (9)$$

In the second stage, the process, starting from level y in phase i , first returns to level y and does so in some phase in \mathcal{S}_2 , and then drains to level zero in phase j . By the physical interpretations of matrices $\hat{\Psi}(s)$ and $Q(s)$ in [8], and Theorem 1 in [10], the Laplace-Stieltjes transform of the second stage is

$$\left[\hat{\Psi}(s) e^{(Q_{22}(s) + Q_{21}(s)\hat{\Psi}(s))y} \right]_{ij}.$$

Premultiplying this by (9) and then integrating with respect to y , gives

$$\begin{aligned} \int_0^\infty e^{-(\vartheta + sc_i^{-1})y} \left(c_i^{-1} \mathcal{T}_{ii} + \vartheta \right) \left[\hat{\Psi}(s) e^{(Q_{22}(s) + Q_{21}(s)\hat{\Psi}(s))y} \right]_{ij} dy = \\ \left[\int_0^\infty e^{-(\vartheta I + sC_1^{-1})y} \left(C_1^{-1} \Delta T_{11} + \vartheta I \right) \hat{\Psi}(s) e^{(Q_{22}(s) + Q_{21}(s)\hat{\Psi}(s))y} dy \right]_{ij}, \end{aligned} \quad (10)$$

where ΔT_{11} is a diagonal matrix with $[\Delta T_{11}]_{ii} = [T_{11}]_{ii}$ for all $i \in \mathcal{S}_1$.

2. Alternatively, in the first stage, the first clock ring occurs at some level y at which point the phase changes to some phase $k \neq i \in \mathcal{S}_1$. In the second stage, the process, starting from level y in phase k , first returns to level y and does so in some phase in \mathcal{S}_2 , and then drains to level zero in phase j . By an argument similar to the first alternative, multiplying the corresponding Laplace-Stieltjes transform, conditioned on the event in the first stage occurring,

$$e^{-s \frac{y}{c_i}}$$

by the probability density of this event

$$\vartheta e^{-\vartheta y \frac{\mathcal{T}_{ik}}{c_i}},$$

then by the Laplace-Stieltjes transform of the second stage,

$$\left[\hat{\Psi}(s) e^{(Q_{22}(s) + Q_{21}(s)\hat{\Psi}(s))y} \right]_{kj},$$

and then integrating with respect to y , we obtain

$$\begin{aligned} \int_0^\infty e^{-(\vartheta + sc_i^{-1})y} \sum_{k \neq i} \left(c_i^{-1} \mathcal{T}_{ik} \right) \left[\hat{\Psi}(s) e^{(Q_{22}(s) + Q_{21}(s)\hat{\Psi}(s))y} \right]_{kj} dy = \\ \left[\int_0^\infty e^{-(\vartheta I + sC_1^{-1})y} \left(C_1^{-1} (T_{11} - \Delta T_{11}) \right) \hat{\Psi}(s) e^{(Q_{22}(s) + Q_{21}(s)\hat{\Psi}(s))y} dy \right]_{ij}. \end{aligned} \quad (11)$$

3. Alternatively, in the first stage, the first clock ring occurs at level y at which point the process moves to some phase $\ell \in \mathcal{S}_0$, spends some time in the set \mathcal{S}_0 and then moves to some phase $k \in \mathcal{S}_1$. In the second stage, the process, starting from level y in phase k , first returns to level y and does so in some phase in \mathcal{S}_2 , and then drains to level zero in phase j . By an argument similar to alternative 2 and step 3 of the proof of [8, Lemma 1], the Laplace-Stieltjes transform of this alternative is

$$\left[\int_0^\infty e^{-(\vartheta I + sC_1^{-1})y} \left(C_1^{-1} T_{10} (T_{00} - sI)^{-1} T_{01} \right) \widehat{\Psi}(s) e^{(Q_{22}(s) + Q_{21}(s)\widehat{\Psi}(s))y} dy \right]_{ij} \quad (12)$$

4. Alternatively, in the first stage, the first clock ring occurs at some level y at which point the process moves to some phase $k \in \mathcal{S}_2$; or to some phase $\ell \in \mathcal{S}_0$, and then spends some time in the set \mathcal{S}_0 and then moves to some phase $k \in \mathcal{S}_2$. In the second stage, the process, starting from level y in phase k , drains to level zero in phase j . The Laplace-Stieltjes transform of this alternative, by an argument similar to alternatives 2 and 3, is

$$\left[\int_0^\infty e^{-(\vartheta I + sC_1^{-1})y} Q_{12}(s) e^{(Q_{22}(s) + Q_{21}(s)\widehat{\Psi}(s))y} dy \right]_{ij} \quad (13)$$

The result follows by summing the matrices corresponding to the four alternatives, given in (10) to (13), and noting that

$$\vartheta I + C_1^{-1} T_{11} + C_1^{-1} T_{10} (T_{00} - sI)^{-1} T_{01} = Q_{11}(s) + (\vartheta I + sC_1^{-1}). \blacksquare$$

Since Algorithm 7 is constructed from (8) by letting $\widehat{\Psi}(s, 0) = 0$ and

$$\begin{aligned} \widehat{\Psi}(s, n+1) &= \int_0^\infty e^{-(\vartheta I + sC_1^{-1})y} \times \\ &\times \left(Q_{12}(s) + \left(Q_{11}(s) + (\vartheta I + sC_1^{-1}) \right) \widehat{\Psi}(s, n) \right) e^{(Q_{22}(s) + Q_{21}(s)\widehat{\Psi}(s, n))y} dy, \end{aligned} \quad (14)$$

the physical interpretation follows. In Algorithm 7, in sample paths contributing to the $(n+1)$ -st iteration, three following stages occur.

- The first stage corresponds to the matrix $e^{-(\vartheta I + sC_1^{-1})y}$. The process $(\widehat{M}(t), \varphi(t))$ starts from level zero in phase $i \in \mathcal{S}_1$, and no clock ring occurs until the level reaches y .
- In the second stage, corresponding to $Q_{12}(s) + \left(Q_{11}(s) + (\vartheta I + sC_1^{-1}) \right) \widehat{\Psi}(s, n)$, either of the following alternatives may occur.
 - In the first alternative, corresponding to $Q_{12}(s)$, the process $(\widehat{M}(t), \varphi(t))$ either makes a single transition to some phase $\ell \in \mathcal{S}_2$; or it makes a single transition to some phase in \mathcal{S}_0 , spends some time in the set \mathcal{S}_0 , and then makes a single transition from the set \mathcal{S}_0 to phase $\ell \in \mathcal{S}_2$.
 - In the second alternative, corresponding to $\left(Q_{11}(s) + (\vartheta I + sC_1^{-1}) \right) \widehat{\Psi}(s, n)$, the process $(\widehat{M}(t), \varphi(t))$ either makes a single transition to some phase in \mathcal{S}_1

(including phase i); or it makes a single transition to some phase in \mathcal{S}_0 , spends some time in the set \mathcal{S}_0 , and then makes a single transition from the set \mathcal{S}_0 to some phase \mathcal{S}_1 . Next, the process first returns to level y and does so in some phase $\ell \in \mathcal{S}_2$. This return path to level y must be in the set $[\Omega_n]_{\nu\mu}$ for some $\nu \in \mathcal{S}_1$ and $\mu \in \mathcal{S}_2$.

- In the third stage, corresponding to $e^{(Q_{22}(s)+Q_{21}(s)\widehat{\Psi}(s,n))y}$, starting from level y in phase $\ell \in \mathcal{S}_2$, the process $(\widehat{M}(t), \varphi(t))$ first drains to level zero and does so in phase j , assuming that, during this stage, any return path to a level $z \in (0, y)$ must be in the set $[\Omega_n]_{\nu\mu}$ for some $\nu \in \mathcal{S}_1$ and $\mu \in \mathcal{S}_2$.

Now, consider the process $(\widehat{M}(t), \varphi(t))$ and introduce yet another way of describing it. First, let $s > 0$. Consider a process with non-conservative generator $\mathcal{T}^* = \mathcal{T} - sI$. We introduce the notation $\widehat{\Psi}^*$, Q^* , Q_{11}^* etc. for this process in order to distinguish it from the notation for the process with generator \mathcal{T} . The following result essentially states that the physical interpretation of Algorithm 9 is derived by applying Algorithm 7 to the problem of calculating hitting probabilities, instead of the Laplace-Stieltjes transforms, of the modified process with generator \mathcal{T}^* .

Lemma 2 *For $s > 0$, matrix $\widehat{\Psi}(s)$ of the process with generator \mathcal{T} is equivalent to matrix $\widehat{\Psi}^*$ of the process with generator \mathcal{T}^* . It follows that*

$$\widehat{\Psi}(s) = \int_0^\infty e^{-\vartheta y} \left(Q_{12}(s) + \left(Q_{11}(s) + \vartheta I \right) \widehat{\Psi}(s) \right) e^{(Q_{22}(s)+Q_{21}(s)\widehat{\Psi}(s))y} dy. \quad (15)$$

Proof First, by [8], $\widehat{\Psi}^*$ is the minimum nonnegative solution of the Riccati equation

$$Q_{12}^* + Q_{11}^* X + X Q_{22}^* + X Q_{21}^* X = 0, \quad (16)$$

and, for $s > 0$, $\widehat{\Psi}(s)$ is the minimum nonnegative solution of

$$Q_{12}(s) + Q_{11}(s)X + X Q_{22}(s) + X Q_{21}(s)X = 0. \quad (17)$$

Since $Q(s) = Q^*$, (16) is equivalent to (17) and hence $\widehat{\Psi}(s) = \widehat{\Psi}^*$.

We can derive (15) directly from the Riccati equation (2). However, we will not do this. On the contrary, we shall determine the first hitting probability of the modified fluid model with generator \mathcal{T}^* by applying the argument used in the proof of Lemma 1 with $s = 0$ to the process with generator \mathcal{T}^* to calculate Ψ^* . That is, for $\vartheta \geq \max_i \{-[C^{-1}\mathcal{T}^*]_{ii}\}$, we assume that a Poisson clock rings at a rate $\vartheta[C]_{ii}$ when the process is in phase i and that state transitions occur according to the transition matrix $P^* = I + (1/\vartheta)Q^*$, and condition on the first clock tick. We obtain

$$\begin{aligned} \widehat{\Psi}^* &= \int_0^\infty e^{-\vartheta y} \left(Q_{12}^* + \left(Q_{11}^* + \vartheta I \right) \widehat{\Psi}^* \right) e^{(Q_{22}^*+Q_{21}^*\widehat{\Psi}^*)y} dy \\ &= \int_0^\infty e^{-\vartheta y} \left(Q_{12}(s) + \left(Q_{11}(s) + \vartheta I \right) \widehat{\Psi}^* \right) e^{(Q_{22}(s)+Q_{21}(s)\widehat{\Psi}^*)y} dy \end{aligned}$$

Hence, the result follows. ■

Algorithm 9 is constructed from (15) by letting $\widehat{\Psi}(s, 0) = 0$ and

$$\begin{aligned} \widehat{\Psi}(s, n+1) &= \int_0^\infty e^{-\vartheta I y} \times \\ &\times \left(Q_{12}(s) + \left(Q_{11}(s) + \vartheta I \right) \widehat{\Psi}(s, n) \right) e^{(Q_{22}(s)+Q_{21}(s)\widehat{\Psi}(s,n))y} dy. \end{aligned} \quad (18)$$

For $s > 0$, the physical interpretation of Algorithm 9 is similar to the physical interpretation of Algorithm 7 in the sense that we condition on the first clock tick, and we split the paths into three stages analogous to the three stages in the physical interpretation of Algorithm 7. However, now the Laplace-Stieltjes transform matrix $\hat{\Psi}(s)$ is calculated by determining the first hitting probability of a modified process. Our numerical experience confirms that the n -th steps of Algorithms 7 and 9, respectively, are not equivalent matrices.

Remark 1 For complex s with $\text{Re}(s) > 0$, we do not have a physical interpretation of Algorithm 9 within the fluid flow model. Instead, we note that, since by [13, Theorem 6.1, page 26] the Laplace-Stieltjes transform is an analytic function, then for all iterations n and phases k and ℓ , the function $h(s; k, \ell, n) \equiv [\hat{\Psi}(s, n)]_{k\ell}$ defined for $s = x + yi$, $x > 0$, is an analytic continuation [19] of the function $g(x; k, \ell, n) \equiv [\hat{\Psi}(x, n)]_{k\ell}$ defined for $x > 0$, and that $\lim_{n \rightarrow \infty} h(s; k, \ell, n)$ is an analytic continuation of $\lim_{n \rightarrow \infty} g(x; k, \ell, n)$. Hence, if $\lim_{n \rightarrow \infty} g(x; k, \ell, n) = [\hat{\Psi}(x)]_{k\ell}$, then $\lim_{n \rightarrow \infty} h(s; k, \ell, n) = [\hat{\Psi}(s)]_{k\ell}$. That is, the convergence of Algorithm 9 for complex s , $\text{Re}(s) > 0$, follows from the convergence for $s > 0$.

3.3 Algorithms 11-14

Since the physical interpretations of the Logarithmic Reduction algorithm [20] and the Cyclic Reduction algorithm [12] are similar, we consider Algorithms 11 and 13 only. We give the physical interpretation of Algorithm 13, the physical interpretation of its dual, Algorithm 11, follows by symmetry. In the lemma below, we show that the n -th iteration of Algorithm 13 is equivalent to the $(2^{n+1} - 1)$ -th iteration of Algorithm 9. Hence, the physical interpretation follows from the physical interpretation of Algorithm 9. Further, we show that n -th iteration of Algorithm 13 produces a matrix equivalent to the n -th iteration of Algorithm 3 in [3].

Lemma 3 *The n -th step of Algorithm 13 yields the matrix*

$$\hat{\Psi}(s, n) = \hat{\Psi}^{(9)}(s, 2^{n+1} - 1),$$

where $\hat{\Psi}^{(9)}(s, 2^{n+1} - 1)$ is the $(2^{n+1} - 1)$ -th iteration of Algorithm 9.

Proof By [20], the matrix G^\bullet in the n -th step of Algorithm 13 is equivalent to $G(2^{n+1} - 1)$, where $G(k+1)$, for $k \geq 0$, is calculated by the linear progression algorithm, in which

$$\begin{aligned} G(0) &= 0, \\ G(k+1) &= \left(I - A'_1(s) - A'_0(s)G(k) \right)^{-1} A'_2(s), \end{aligned} \quad (19)$$

where $G(k)$, for $k \geq 0$, partitioned in a way analogous to $P(s)$, is of the form

$$G(k) = \begin{bmatrix} 0 & X_k \\ 0 & Y_k \end{bmatrix}. \quad (20)$$

Define $\hat{F}(s, k) = P_{11}(s)X_k + P_{12}(s)Y_k$. Then, the n -th iteration of Algorithm 13 yields the matrix $\hat{\Psi}(s, n) = \hat{F}(s, 2^{n+1} - 1)$. Next, we show that $\hat{F}(s, k)$, for all $k \geq 0$, is

equivalent to the k -th iteration of Algorithm 9, which completes the proof. Clearly, this assertion is true for $k = 0$. Assume that it is true for some k .

By writing the recursive formula (19) for $G(k+1)$ in the form

$$\left(I - A_1'(s) - A_0'(s)G(k) \right) G(k+1) = A_2'(s)$$

and then substituting all the matrices in (7), and in (20) for k and $(k+1)$, we obtain

$$\begin{bmatrix} 0 & X_{k+1} - P_{11}(s)X_k Y_{k+1} - P_{12}(s)Y_k Y_{k+1} \\ 0 & -\frac{1}{2}P_{21}(s)X_{k+1} + Y_{k+1} - \frac{1}{2}P_{22}(s)Y_{k+1} \end{bmatrix} = \begin{bmatrix} 0 & 0 \\ 0 & \frac{1}{2}I \end{bmatrix}.$$

Comparing the left and the right hand sides of this equation gives

$$\begin{aligned} X_{k+1} &= \left(P_{11}(s)X_k + P_{12}(s)Y_k \right) Y_{k+1} \\ &= \widehat{\Gamma}(s, k)Y_{k+1}, \end{aligned}$$

and

$$\begin{aligned} I &= -P_{21}(s)X_{k+1} + 2Y_{k+1} - P_{22}(s)Y_{k+1} \\ &= -P_{21}(s)\widehat{\Gamma}(s, k)Y_{k+1} + 2Y_{k+1} - P_{22}(s)Y_{k+1} \\ &= \left(-P_{21}(s)\widehat{\Gamma}(s, k) + 2I - P_{22}(s) \right) Y_{k+1}, \end{aligned}$$

and so

$$Y_{k+1} = \left(2I - P_{22}(s) - P_{21}(s)\widehat{\Gamma}(s, k) \right)^{-1}.$$

Consequently,

$$\begin{aligned} \widehat{\Gamma}(s, k+1) &= P_{11}(s)X_{k+1} + P_{12}(s)Y_{k+1} \\ &= P_{11}(s)\widehat{\Gamma}(s, k)Y_{k+1} + P_{12}(s)Y_{k+1} \\ &= \left(P_{11}(s)\widehat{\Gamma}(s, k) + P_{12}(s) \right) \left(2I - P_{22}(s) - P_{21}(s)\widehat{\Gamma}(s, k) \right)^{-1} \\ &= \left(\left(I + \frac{1}{\vartheta}Q_{11}(s) \right) \widehat{\Gamma}(s, k) + \frac{1}{\vartheta}Q_{12}(s) \right) \times \\ &\quad \times \left(2I - \left(I + \frac{1}{\vartheta}Q_{22}(s) \right) - \frac{1}{\vartheta}Q_{21}(s)\widehat{\Gamma}(s, k) \right)^{-1} \\ &= \left(Q_{12}(s) + \left(Q_{11}(s) + \vartheta I \right) \widehat{\Gamma}(s, k) \right) \times \frac{1}{\vartheta} \times \\ &\quad \times \left(\vartheta I - Q_{22}(s) - Q_{21}(s)\widehat{\Gamma}(s, k) \right)^{-1} \times \left(\frac{1}{\vartheta} \right)^{-1} \end{aligned}$$

which is equivalent to the $(k+1)$ -st iteration of Algorithm 9. By induction, the result follows. ■

Let $\widehat{\Psi}^*(s, n)$ be the approximation of $\widehat{\Psi}(s)$ obtained after n iterations of Algorithm 3 in [3]. Below, we show that the matrices $\widehat{\Psi}^*(s, n)$ and $\widehat{\Psi}(s, n)$ are equivalent. Note that both Algorithm 13 and Algorithm 3 in [3] use the Logarithmic Reduction algorithm [20]. However, they each use a *different* set of input matrices. Algorithm 13 incorporates the effect of excursions to \mathcal{S}_0 in \mathcal{S}_1 and \mathcal{S}_2 , and hence is more efficient (see Section 4 for the details).

Lemma 4 *The n -th step of Algorithm 13 satisfies the equivalence*

$$\widehat{\Psi}(s, n) = \widehat{\Psi}^*(s, n).$$

Proof Let $P = \vartheta^{-1}C^{-1}\mathcal{T} + I$ be partitioned according to $\mathcal{S} = \mathcal{S}_1 \cup \mathcal{S}_2 \cup \mathcal{S}_0$. Algorithm 3 in [3], after n iterations, yields the following approximation of the matrix $\widehat{\Psi}(s)$ (in our notation):

$$\widehat{\Psi}^*(s, n) = (P_{11} - \frac{s}{\vartheta}C_1^{-1})X_n^* + P_{12}Y_n^* + P_{10}Z_n^*,$$

where the matrix

$$G(s, \vartheta, n) = \begin{bmatrix} 0 & X_n^* & 0 \\ 0 & Y_n^* & 0 \\ 0 & Z_n^* & 0 \end{bmatrix}$$

is obtained by applying the Logarithmic Reduction algorithm [20] to the following set of matrices:

$$\begin{aligned} A_0^* &= \begin{bmatrix} P_{11} - \frac{s}{\vartheta}C_1^{-1} & P_{12} & P_{10} \\ 0 & 0 & 0 \\ 0 & 0 & 0 \end{bmatrix} \\ A_1^* &= \begin{bmatrix} 0 & 0 & 0 \\ \vartheta C_2(2\vartheta C_2 + sI)^{-1}P_{21} & C_2(2\vartheta C_2 + sI)^{-1}P_{22} & C_2(2\vartheta C_2 + sI)^{-1}P_{20} \\ \frac{\vartheta}{\vartheta+s}P_{01} & \frac{\vartheta}{\vartheta+s}P_{02} & \frac{\vartheta}{\vartheta+s}P_{02} \end{bmatrix} \\ A_2^* &= \begin{bmatrix} 0 & 0 & 0 \\ 0 & \vartheta C_2(sI + 2\vartheta C_2)^{-1} & 0 \\ 0 & 0 & 0 \end{bmatrix}. \end{aligned} \tag{21}$$

By [20], $G(s, \vartheta, n)$ is equivalent to $G^{**}(2^{n+1} - 1)$, where $G^{**}(k+1)$, for $k \geq 0$ is calculated by the linear progression algorithm, in which

$$\begin{aligned} G^{**}(0) &= 0, \\ G^{**}(k+1) &= \left(I - A_1^* - A_0^*G^{**}(k) \right)^{-1} A_2^*, \end{aligned}$$

where $G^{**}(k)$, for $k \geq 0$, is of the form

$$G^{**}(k) = \begin{bmatrix} 0 & X_n^{**} & 0 \\ 0 & Y_n^{**} & 0 \\ 0 & Z_n^{**} & 0 \end{bmatrix}.$$

Define $\widehat{\Gamma}(s, k) = (P_{11} - \frac{s}{\vartheta}C_1^{-1})Z_k^{**} + P_{12}Y_k^{**} + P_{10}Z_k^{**}$. The proof of the fact that $\widehat{\Gamma}(s, k)$, for all $k \geq 0$, is equivalent to the k -th iteration of Algorithm 9, follows in a manner analogous to the proof of Lemma 3. ■

3.4 Convergence

Theorem 1 For s , with $\operatorname{Re}(s) > 0$, $\hat{\Psi}(s, n) \rightarrow \hat{\Psi}(s)$ as $n \rightarrow \infty$, for each of Algorithms 1-14.

Proof For Algorithms 1-8, the result follows from the physical interpretations, by noting that, for all n , any sample path contributing to $\hat{\Psi}(s, n)$ must contribute to $\hat{\Psi}(s)$, and any sample path contributing to $\hat{\Psi}(s)$ must contribute to $\hat{\Psi}(s, n)$ for some n . The convergence for Algorithms 9-14 for $s > 0$ follows by an analogous argument. The convergence for Algorithms 9-14 for complex s , $\operatorname{Re}(s) > 0$, follows by the analytic continuation argument in Remark 1. \blacksquare

From the physical interpretations above it follows by [9] that the convergence of Algorithm 4 is R -quadratic [21], while the convergence of Algorithms 1-3, and 5-6 is R -linear [21], and the convergence of Algorithms 7-8 is at most R -linear. By [20], the convergence of Algorithms 11-14 is R -quadratic while the convergence of Algorithms 9-10 is R -linear.

4 Numerical complexity

The numerical complexity of an algorithm depends on the complexity per iteration and the number of iterations required for the algorithm to converge. These two parameters are analyzed here for each of the algorithms 1-14. The size of the set \mathcal{S}_0 does not affect the complexity of these algorithms. We assume that the equations of type $AX + XB = -C$ in Algorithms 1-4 are solved using the Bartels-Stewart algorithm [6]. Let \mathcal{W}_k be the complexity of the n -th iteration, $n \geq 2$, for Algorithm k , $k \in \{1, \dots, 14\}$. Let $|\mathcal{S}_1 \cup \mathcal{S}_2| = r$. By [9, 20], when $|\mathcal{S}_1| = |\mathcal{S}_2| = r/2$, we have

$$\begin{aligned}\mathcal{W}_1 &\approx \frac{7}{4}r^3, \\ \mathcal{W}_2 &= \mathcal{W}_3 \approx 4r^3, \\ \mathcal{W}_4 &\approx \frac{29}{4}r^3, \\ \mathcal{W}_5 &= \mathcal{W}_6 \approx \frac{1}{6}r^4, \\ \mathcal{W}_7 &= \mathcal{W}_8 \approx \frac{27}{8}r^3, \\ \mathcal{W}_9 &= \mathcal{W}_{10} \approx \frac{1}{3}r^3, \\ \mathcal{W}_{11} &= \mathcal{W}_{13} \approx \frac{50}{3}r^3, \\ \mathcal{W}_{12} &= \mathcal{W}_{14} \approx \frac{44}{3}r^3.\end{aligned}$$

These complexities can be different when $|\mathcal{S}_1| \neq |\mathcal{S}_2|$. For example, by [9], when $|\mathcal{S}_1|$ is small but $|\mathcal{S}_2|$ is large, then $\mathcal{W}_2 > \mathcal{W}_3$. However, the complexities of Algorithms 11 to 14 depend only on the size of the set $\mathcal{S}_1 \cup \mathcal{S}_2$. The complexity per iteration of Algorithm 3 in [3], where $q = |\mathcal{S}_0|$, is

$$\mathcal{W}^* \approx \frac{50}{3}(r + q)^3,$$

and so may be much higher than the complexity of Algorithm 13, depending on the size of the set \mathcal{S}_0 .

Let N_k be the number of iterations required for Algorithm k to converge, for $k \in \{1, \dots, 14\}$, respectively. By the physical interpretations of the algorithms given in Section 3, we conclude that

$$\begin{aligned} N_1 &\geq N_2 \geq N_4, \\ N_1 &\geq N_3 \geq N_4, \\ N_7 &\geq N_5, \\ N_8 &\geq N_6, \\ N_9 &\geq N_{13}, \\ N_{10} &\geq N_{11}, \\ N_{12} &\geq N_{11}, \\ N_{14} &\geq N_{13}. \end{aligned}$$

Our numerical experience suggests that Algorithm 4 requires no more iterations than any of the Algorithms 10-14. It seems that, theoretically, Algorithm 4 is the best performer. As pointed out in [9], and as we also observe in the next section, the implementation of this algorithm is slightly more difficult, however.

5 Numerical performance

We have implemented all the algorithms in MATLAB, with $\epsilon = 10^{-12}$. We put an upper bound of 100 iterations on each algorithm. Average CPU times were obtained by running each algorithm 100 times.

Table 1 Data for Example 1.

| Algorithm | Number of iterations | Average CPU time |
|-----------|----------------------|------------------|
| 1 | 46 | 0.01590 |
| 2 | 29 | 0.01154 |
| 3 | 29 | 0.01176 |
| 4 | 6 | 0.00282 |
| 5 | 43 | 0.01237 |
| 6 | 43 | 0.01249 |
| 7 | 43 | 0.01998 |
| 8 | 43 | 0.01968 |
| 9 | 41 | 0.00672 |
| 10 | 41 | 0.00660 |
| 11 | 7 | 0.00202 |
| 12 | 8 | 0.00219 |
| 13 | 7 | 0.00250 |
| 14 | 8 | 0.00312 |

As in [9], we observe that the performance of the algorithms depends on the nature of the stochastic fluid flow process under consideration. Note that, theoretically, Algorithm 4 should perform much better, but this theoretical advantage is not reflected

here, we believe due to the inherent optimisation features of MATLAB. Nevertheless, Algorithm 4 consistently requires the smallest number of iterations. We have highlighted the outputs corresponding to this algorithm for easy comparison with other algorithms.

Example 1 Let $s = 2 + i$. Consider the process with

$$\mathcal{T} = \left[\begin{array}{cc|cc} -30 & 10 & 10 & 10 \\ 10 & -30 & 10 & 10 \\ \hline 10 & 10 & -30 & 10 \\ 10 & 10 & 10 & -30 \end{array} \right].$$

The outcome of using the various algorithms is given in Table 1. Algorithms 1 to 3 and 5 to 10 require a large number of iterations and their CPU times are much higher than the CPU times for the algorithms 4 and 11 to 14.

Example 2 Let $s = 2 + i$. Consider the process with

$$\mathcal{T} = \left[\begin{array}{cc|cc} -102 & 100 & 1 & 1 \\ 100 & -102 & 1 & 1 \\ \hline 1 & 1 & -3 & 1 \\ 1 & 1 & 1 & -3 \end{array} \right].$$

The outcome is given in Table 2. Algorithm 4 requires the least number of iterations and has the smallest CPU time. Algorithms 5 and 7 to 10 did not converge in the 100 iterations.

Table 2 Data for Example 2.

| Algorithm | Number of iterations | Average CPU time |
|-----------|----------------------|------------------|
| 1 | 13 | 0.00500 |
| 2 | 11 | 0.00468 |
| 3 | 11 | 0.00455 |
| 4 | 5 | 0.00202 |
| 5* | — | — |
| 6* | 16 | 0.00483 |
| 7* | — | — |
| 8* | — | — |
| 9* | — | — |
| 10* | — | — |
| 11 | 10 | 0.00325 |
| 12 | 11 | 0.00327 |
| 13 | 10 | 0.00363 |
| 14 | 11 | 0.00423 |

*The algorithm did not converge in the 100 iterations.

Example 3 Let (a) $s = 2 + i$, or (b) $s = i$. Consider the process with $|\mathcal{S}_1|=2$, $|\mathcal{S}_2| = 18$, and with off-diagonal entries in \mathcal{T}_{11} equal to 0, all entries in \mathcal{T}_{12} equal to 0.001, all entries in \mathcal{T}_{21} equal to 0.001, and all off-diagonal entries in \mathcal{T}_{22} equal to 10. The outcome is given in Table 3. Note that, although Algorithms 11 to 14 are quadratically convergent,

Table 3 Data for Example 3 (a) $s = 2 + i$ (b) $s = i$, respectively.

| Algorithm | Number of iterations | Average CPU time |
|-----------|----------------------|------------------|
| 1 | 3 | 0.00889 |
| 2 | 3 | 0.00842 |
| 3 | 3 | 0.01002 |
| 4 | 3 | 0.00936 |
| 5 | 5 | 0.00420 |
| 6 | – | – |
| 7* | – | – |
| 8* | – | – |
| 9* | – | – |
| 10* | – | – |
| 11 | 11 | 0.02183 |
| 12 | 12 | 0.02312 |
| 13 | 11 | 0.02798 |
| 14 | 12 | 0.03052 |

*The algorithm did not converge in the 100 iterations.

| Algorithm | Number of iterations | Average CPU time |
|-----------|----------------------|------------------|
| 1 | 3 | 0.00829 |
| 2 | 3 | 0.00988 |
| 3 | 3 | 0.00770 |
| 4 | 3 | 0.01061 |
| 5 | 6 | 0.00339 |
| 6 | – | – |
| 7* | – | – |
| 8* | – | – |
| 9* | – | – |
| 10* | – | – |
| 11 | 19 | 0.03844 |
| 12 | 20 | 0.04041 |
| 13 | 19 | 0.04146 |
| 14 | 20 | 0.04483 |

*The algorithm did not converge in the 100 iterations.

the number of iterations for them is high in this strongly recurrent process! Algorithm 5 is the best performer here. This is because of the small complexity per iteration for this algorithm due to small $|\mathcal{S}_1|$, and the small number of iterations due to zero off-diagonal entries in \mathcal{T}_{11} . Algorithms 6 to 10 did not converge in the 100 iterations.

Example 4 Let $s = i$. Consider the process with $|\mathcal{S}_1|=18$, $|\mathcal{S}_2| = 2$, and with off-diagonal entries in Q_{22} equal to 0, all entries in Q_{21} equal to 0.001, all entries in Q_{12} equal to 0.001, and all off-diagonal entries in Q_{11} equal to 10. The outcome is given in Table 4. As in Example 3, the number of iterations for Algorithms 11-14 is high in this strongly transient process. Algorithms 6 to 10 did not converge in the 100 iterations. Algorithm 2 is the best performer here.

Table 4 Data for Example 4.

| Algorithm | Number of iterations | Average CPU time |
|-----------|----------------------|------------------|
| 1 | 3 | 0.01062 |
| 2 | 3 | 0.00500 |
| 3 | 3 | 0.01174 |
| 4 | 3 | 0.00529 |
| 5 | 3 | 0.01107 |
| 6 | – | – |
| 7* | – | – |
| 8* | – | – |
| 9* | – | – |
| 10* | – | – |
| 11 | 15 | 0.03064 |
| 12 | 16 | 0.03232 |
| 13 | 15 | 0.03094 |
| 14 | 16 | 0.03172 |

*The algorithm did not converge in the 100 iterations.

Example 5 Let $s = 2 + i$. Consider the processes with

$$(a) \mathcal{T} = \left[\begin{array}{cc|ccc} -2 & 0 & 2 & 0 & 0 \\ 0 & -100 & 100 & 0 & 0 \\ \hline 0 & 0 & -3 & 3 & 0 \\ 0 & 0 & 0 & -3 & 3 \\ 1.5 & 1.5 & 0 & 0 & -3 \end{array} \right], \quad (b) \mathcal{T} = \left[\begin{array}{ccc|cc} -3 & 3 & 0 & 0 & 0 \\ 0 & -3 & 3 & 0 & 0 \\ \hline 0 & 0 & -3 & 1.5 & 1.5 \\ 2 & 0 & 0 & -2 & 0 \\ 100 & 0 & 0 & 0 & -100 \end{array} \right].$$

Algorithm 4 is the best performer here. This example has been constructed to illustrate the fact that the number of iterations required in the dual algorithms may not be the same. Of course, for a sample path to be included in $\hat{\Psi}(s)$ the total length of the “upwards” part and of the “downwards” part must be the same. Also, the number of upward and downward sections also must be the same. Therefore, the conditional mean length of each upward part must be the same as that of each downward part. Therefore, to exhibit the difference between the dual algorithms, we need to make the conditional distribution of the upward parts to be different to that of the downward parts. Accordingly, we chose to have an Erlang order 3 distribution for the downward parts and a very high coefficient of variation Hyper-Exponential distribution for the upward parts, in (a). In (b) we interchanged these.

In (a), Algorithm 5 performs better than Algorithm 6 and Algorithm 2 performs better than Algorithm 3, but the reverse is true in (b). Although $N_{11} = N_{13}$ and $N_{12} = N_{14}$, the errors obtained are different (since the errors for Algorithms 9 and 10 are different), and so clearly the corresponding dual algorithms are not equivalent either.

Summarizing, we observe that the performance of the algorithms depends on the processes studied. Algorithms which perform well in some cases, may not perform well in others. An algorithm and its dual may each perform differently in different cases. Quadratic Algorithms 11 to 14 may perform worse than other linear algorithms, even when a process considered is strongly positive recurrent. Algorithm 4 is the most reliable algorithm overall and we recommend using it for the calculation of $\hat{\Psi}(s)$.

Table 5 Data for Example 5 (a) and (b), respectively.

| Algorithm | Number of iterations | Average CPU time |
|-----------|----------------------|------------------|
| 1 | 9 | 0.00426 |
| 2 | 7 | 0.00393 |
| 3 | 9 | 0.00498 |
| 4 | 4 | 0.00297 |
| 5 | 7 | 0.00202 |
| 6 | 22 | 0.00923 |
| 7* | — | — |
| 8* | — | — |
| 9* | — | — |
| 10* | — | — |
| 11 | 10 | 0.00373 |
| 12 | 11 | 0.00436 |
| 13 | 10 | 0.00372 |
| 14 | 11 | 0.00392 |

*The algorithm did not converge in the 100 iterations.

| Algorithm | Number of iterations | Average CPU time |
|-----------|----------------------|------------------|
| 1 | 9 | 0.00438 |
| 2 | 9 | 0.00408 |
| 3 | 7 | 0.00390 |
| 4 | 4 | 0.00327 |
| 5 | 22 | 0.00795 |
| 6 | 7 | 0.00295 |
| 7* | — | — |
| 8* | — | — |
| 9* | — | — |
| 10* | — | — |
| 11 | 10 | 0.00325 |
| 12 | 11 | 0.00421 |
| 13 | 10 | 0.00362 |
| 14 | 11 | 0.00473 |

*The algorithm did not converge in the 100 iterations.

6 Application to Calculating Densities

Let $\psi(t)_{ij}$ be the probability density of first return to the initial level being at time t and in phase $j \in \mathcal{S}_2$, assuming that the process starts in phase $i \in \mathcal{S}_1$, while avoiding levels below zero. That is,

$$[\widehat{\Psi}(s)]_{ij} = \int_0^\infty e^{-st} \psi(t)_{ij} dt.$$

Since $\Psi(s)$ can be efficiently calculated using any of the quadratic algorithms described in this paper, we can apply the method of Abate and Whitt in [1] for the numerical inversion of Laplace transforms in order to obtain $\psi(t)$ from $\Psi(s)$, for $t > 0$. Here, we choose to apply Algorithm 4 due to its consistently reliable numerical performance, and implement our method using MATLAB. As an illustration, we calculate the probability densities $[\psi(t)]_{ij}$ for a couple of simple stochastic fluid processes below.

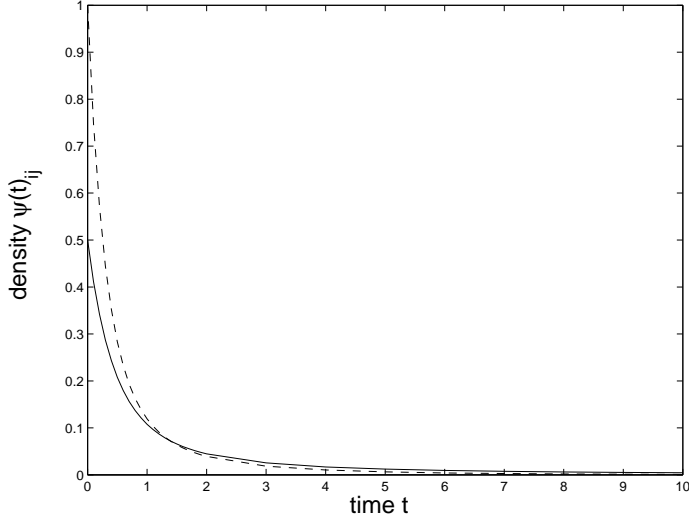


Fig. 1 Null-recurrent (solid line) and positive-recurrent processes.

Example 6 Let $\mathcal{S}_1 = \{1, 2\}$, $\mathcal{S}_2 = \{3, 4\}$, $C_1 = C_2 = I$. Consider a positive-recurrent process and a null-recurrent process with generators

$$\mathcal{T} = \left[\begin{array}{cc|cc} -5 & 1 & 2 & 2 \\ 1 & -5 & 2 & 2 \\ \hline 1 & 1 & -4 & 2 \\ 1 & 1 & 2 & -4 \end{array} \right] \text{ and } \mathcal{T}' = \left[\begin{array}{cc|cc} 1 & 1 & -3 & 1 \\ 1 & 1 & 1 & -3 \\ \hline -3 & 1 & 1 & 1 \\ 1 & -3 & 1 & 1 \end{array} \right],$$

respectively. After running our algorithm for various values, we noticed that the values of $\psi(t)_{ij}$ are very close to zero for $t \geq 10$, and so we restricted the range of our graph to the interval $(0, 10]$. In order to obtain the desired smoothness of the graph, we plotted more points in the time interval $(0, 2]$ than in the rest of the range. The results are illustrated in Figure 1. Note that, due to the symmetry, the graphs are the same for all $i \in \mathcal{S}_1$ and $j \in \mathcal{S}_2$. Observe that the area under $\psi(t)_{ij}$ for both processes is equal to 0.5^1 , which can be confirmed by calculating $\Psi_{ij} = \int_0^\infty \psi(t)_{ij} dt$ using any of the algorithms for $\Psi(s)$ described in this paper (simply set $s = 0$ in those algorithms). Note also that in the null-recurrent process, the convergence of $\psi(t)_{ij}$ to zero, as $t \rightarrow \infty$, is slower than in the positive-recurrent process.

7 Conclusion

We have derived and analyzed several algorithms, including five quadratically convergent algorithms for the matrix $\hat{\Psi}(s)$, which records the Laplace-Stieltjes transforms of the time taken to return to the initial level, in the fluid flow model. We have provided useful physical interpretations of all the algorithms in terms of the fluid flow model, and proved the convergence using these interpretations. We have analyzed the numerical

¹ Note the process is equally likely to first return to level 0 in both states and so the total return probability is 1, as expected.

complexities of the algorithms and given several simple numerical examples, in which we compared the algorithms with respect to their performance. We have presented the application of these results to calculating the probability density of the time taken to return to the initial level.

References

1. J. Abate and W. Whitt, Numerical inversion of Laplace Transforms of probability distributions, *ORSA Journal on Computing*, **7**(1), 36–43 (1995).
2. S. Ahn and V. Ramaswami, Transient analysis of fluid flow models via stochastic coupling to a queue, *Stochastic Models*, **20**(1), 71–101 (2004).
3. S. Ahn and V. Ramaswami, Efficient algorithms for transient analysis of stochastic fluid flow models, *Journal of Applied Probability*, **42**(2), 531–549 (2005).
4. S. Ahn and V. Ramaswami, Matrix-geometric algorithms for stochastic fluid flows, *ACM International Conference Proceedings Series*, Proceedings from the 2006 workshop on Tools for solving structured Markov Chains (2001).
5. S. Asmussen, Stationary distributions for fluid flow models with or without Brownian noise, *Stochastic Models*, **11**, 21–49 (1995).
6. R. H. Bartels and G. W. Stewart, Algorithm 432: Solution of the matrix equation $AX+XB=C$, *Communications of the ACM*, **15**(9), 820–826 (1972).
7. N.G. Bean and M.M. O'Reilly, Performance Measures of a Fluid Flow Model with an Element of Level Dependence, Submitted.
8. N.G. Bean, M.M. O'Reilly and P.G. Taylor, Hitting probabilities and hitting times for stochastic fluid flows, *Stochastic Processes and Their Applications*, **115**(9), 1530–1556 (2005).
9. N.G. Bean, M.M. O'Reilly and P.G. Taylor, Algorithms for return probabilities for stochastic fluid flows, *Stochastic Models*, **21**(1), 149–184 (2005).
10. N.G. Bean and M.M. O'Reilly, Hitting probabilities and hitting times for stochastic fluid flows in the bounded model, Submitted.
11. R. Bwidehatia and P. Rosenthal, How and why to solve the operator equation $AX - XB = Y$, *Bulletin of the London Mathematical Society*, **29**, 1–21 (1997).
12. D. Bini and B. Meini, On the solution of a nonlinear matrix equation arising in queueing problems, *SIAM Journal on Matrix Analysis and Applications*, **17**(4), 906–926 (1996).
13. G. Doetsch, translated from German by W. Nader, *Introduction to the Theory and Application of the Laplace Transformation*. Springer Verlag, Berlin (1974).
14. A. Da Silva Soares and G. Latouche, Further results on the similarity between fluid queues and QBDs. In G. Latouche and P. Taylor, editors, *Matrix-Analytic Methods Theory and Applications*, pages 89–106, World Scientific Press (2002).
15. A. Da Silva Soares and G. Latouche, Matrix-analytic methods for fluid queues with finite buffers, *Performance Evaluation*, **63**, 295–314 (2006).
16. G. H. Golub, S. Nash and C. Van Loan, A Hessenberg-Schur method for the problem $AX + XB = C$, *IEEE Transactions on Automatic Control*, **AC-24**(6), 909–913 (1979).
17. C-H. Guo, Nonsymmetric algebraic Riccati equations and Wiener-Hopf factorization for M-matrices, *SIAM Journal on Matrix Analysis and Applications*, **23**(1), 225–242 (2001).
18. A. Jensen, *Markoff Chains as an aid in the study of Markoff processes*, Skand. Aktuariestidskr., **36**, 87–91 (1953).
19. Knopp K, *Theory of functions*. Dover Publications, New York (1945).
20. G. Latouche and V. Ramaswami, *Introduction to matrix analytic methods in stochastic modeling*. American Statistical Association and SIAM, Philadelphia (1999).
21. J. M. Ortega and W. C. Rheinboldt, *Iterative solution of nonlinear equations in several variables*. Academic Press, New York (1970).
22. V. Ramaswami, Matrix analytic methods for stochastic fluid flows, *Proceedings of the 16th International Teletraffic Congress*, Edinburgh, 7-11 June 1999, pages 1019–1030 (1999).